General palaeontology

Homo erectus from the Yunxian and Nankin Chinese sites: Anthropological insights using 3D virtual imaging techniques

Étude des Homo erectus de Yunxian et de Nankin en Chine. Apport de l'imagerie 3D

Amélie Vialet [a],[*], Gaspard Guipert [b], He Jianing [c], Feng Xiaobo [d], Lu Zune [c], Wang Youping [c], Li Tianyuan [e], Marie-Antoinette de Lumley [a], Henry de Lumley [a]

[a] Institut de paléontologie humaine, fondation Albert-Ier-de-Monaco, 1, rue René-Panhard, 75013 Paris, France
[b] Antenne de l'institut de paléontologie humaine, CEREGE, Europôle de l'Arbois, bâtiment Villemin, BP 80, 13145 Aix-en-Provence, France
[c] Department of Archaeology, University of Beijing, 100871 Beijing, China
[d] Institute of Vertebrate Paleontology and Paleoanthropology, Chinese Academy of Sciences, 100044 Beijing, China
[e] Archaeological and Cultural Relics Institute of Hubei, 81, Tian'e Donghu Road, 43077 Wuhan, China

ARTICLE INFO

ABSTRACT

Recent applications of 3D virtual imaging techniques in human palaeontology have increased the possibilities and the accuracy of anthropological analysis. Two examples are given for the reconsideration of fossils discovered more than 20 years ago, thanks to this new technology. The Lower and Middle Pleistocene skulls from Yunxian and Nankin in China, which were damaged in the process of fossilization, have been virtually reconstructed. A detailed reinvestigation has been conducted by considering those reconstructed skulls and their unpublished characters (i.e., inner anatomical features inaccessible until now). The results of this analysis provide new information about the early hominids of China and contribute to the discussion of variability in Homo erectus.

© 2010 Académie des sciences. Published by Elsevier Masson SAS. All rights reserved.

RÉSUMÉ

Récemment appliquée à la paléontologie humaine, l'imagerie tridimensionnelle a considérablement augmenté les possibilités et le degré de précision des analyses paléoanthropologiques. Deux exemples sont donnés de la reprise, grâce à cette technologie, de l'étude de fossiles découverts il y a plus de 20 ans. Les crânes de Yunxian et de Nankin, respectivement du Pléistocène inférieur et moyen de Chine, altérés au cours de leur fossilisation, ont été virtuellement reconstitués. Une investigation a pu être réalisée sur ces crânes reconstitués, devenus plus complets, en intégrant les caractères inédits, c'est-à-dire les caractères anatomiques internes jusqu'alors inaccessibles. Les résultats de cette étude donnent des informations sur les premiers hominidés de Chine et apportent de nouveaux éléments dans la discussion sur la variabilité de l'espèce Homo erectus.

© 2010 Académie des sciences. Publié par Elsevier Masson SAS. Tous droits réservés.

* Corresponding author.
E-mail address: amelievialet@fondationiph.org (A. Vialet).

1. Introduction

For the last decades, 3D virtual imaging techniques have opened new paths in palaeoanthropology (for the first applications: e.g. Balzeau et al., 2002; Braun, 1996; Conroy et al., 2000; Macchiarelli et al., 1999; Mafart and Delingette, 2002; Seidler et al., 1997; Spoor et al., 2003; Thompson and Illerhaus, 1998; Zollikofer et al., 1995, and, for the latest contributions: e.g. Balzeau and Rougier, 2010; Bayle et al., 2009; Bruner and Manzi, 2008; Falk et al., 2009; Gilbert and Asfaw, 2009; Hill and Richtsmeier, 2008; Olejniczak et al., 2008; Poza-Rey and Arsuaga, 2009). The fossils discovered, often a long time ago, too crushed or damaged to be studied, can now be reconstructed and integrated in comparative studies (e.g. Berge and Goularas, 2010; Guipert et al., 2007; Mafart et al., 2007; Manzi et al., 2001; Ponce de Leon and Zollikofer, 1999; Sémal et al., 2005; Sylvester et al., 2008; Zollikofer et al., 2005).

In China, although palaeoanthropological discoveries have increased recently (Shang et al., 2007; Wu et al., 2008; Xing et al., 2009), fossil hominid remains are still rare. Among them, the Lower Pleistocene specimen from the Yunxian site, on the one hand, and the Middle Pleistocene specimen from the Hulu Cave, near Nankin, on the other hand, constitute key-fossils to improve our knowledge on the first hominids of China. As one suffered from plastic deformation and the other was too fragmentary, virtual reconstruction of those two skulls was carried out. Thanks to this reconstruction, a further and more detailed anthropological analysis could be done. Standard anthropological analysis, as well as a 3D morphometric geometric approach, were managed. Results are discussed in the context of the discussion on the variability of the species *Homo erectus*.

2. Material

2.1. The Yunxian fossils

The Yunxian site is located on a terrace which corresponds to the highest alluvial formation (219 m) of the Han River, a tributary of the Blue River in the Hubei Province, at 550 km north-east of Wuhan and 40 km west of Yunxian. Excavated in the 1990s, the archaeological layer No. 3 has yielded faunal remains and lithic industry as well as two hominid skulls with calcareous encrusting (Etler and Li, 1994; Li and Etler, 1992; Li and Feng, 2001).

Thanks to the French and Chinese collaboration managed by Professor Henry de Lumley and Professor Li Tianyuan, a pluridisciplinary research program has been developed leading to new results. The biostratigraphical correlations between the Yunxian and the Lantian-Gongwangling site, dated by means of magnetostratigraphy and lithostratigraphy at around 1.15 Myr (Zhu et al., 2003), have first given an idea of the great antiquity of the Yunxian site. Moreover, analysis using Uranium series and Electronic Spin Resonance (RPE) on some teeth of the Yunxian fauna, has yielded a mean age of about 600,000 years (Chen et al., 1997). To end, a geochronological work has identified, within the layer No. 3, the Santa Rosa geomagnetic excursion which corresponds to a short period of nor-
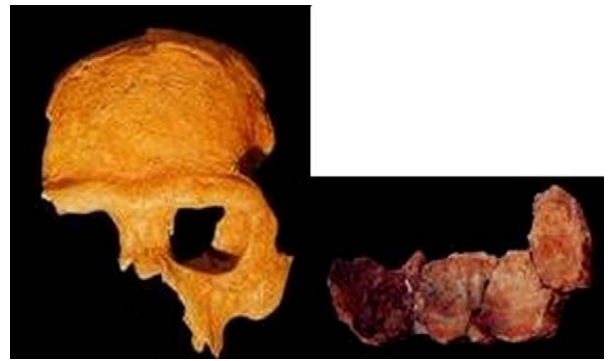

Fig. 1. Nankin 1a (on the left) and Nankin 1b and 1c (on the right). Note that the bones (Nankin 1b and 1c) were placed in anatomical connexion.
Fig. 1. Nankin 1a (à gauche) et Nankin 1b et 1c (à droite). À noter que les spécimens (Nankin 1b et 1c) ont été placés en connexion anatomique pour les besoins de la photographie.

mal polarity in the long Matuyama reverse sequence, giving an accurate age of 936,000 years (de Lumley et al., 2008a).

2.2. The Nankin fossils

The Hulu Cave is situated near Tangshan, at 26 km east of Nankin (Tangshan), in the Jiangsu Province. In 1993, during alterations in the cave, three human remains (Nankin 1) were discovered (Fig. 1). Further research has uncovered one supplementary partial skullcap (Nankin 2) and one isolated molar (Nankin 3). Although the circumstances of these discoveries are not well known, datings gave a Middle Pleistocene age (Lu, 1996; Wu et al., 2002). Due to the evidences of the presence of hyena and the absence of lithic industry associated with the human remains, the cave is regarded as having been a den of hyenas. Nankin 1 specimen has three fragments (designated for convenience in the present paper as Nankin 1a, Nankin 1b, Nankin 1c). The best preserved (Nankin 1a) is composed of a nearly complete frontal bone, half of the left parietal and a supero-anterior fragment of the right parietal and a nearly entire left part of the face (orbit, cheek bone, infra-orbital part including the frontal and maxillary processes). An isolated occipital fragment corresponding to the transverse occipital torus area still in connexion with a fragment of the left parietal bone (Nankin 1b) and a fragment of the right parietal (Nankin 1c) are also preserved (Fig. 1).

2.3. The reference samples

Casts of the fossil hominids and modern human skulls used as reference samples are from the collection of the *Institut de paléontologie humaine*. The African adult skulls assigned to *Homo ergaster*: KNM-ER3733 and 3883 were considered as well as the following European fossils from Middle and Upper Pleistocene: Petralona, La Quina H5 and La Ferrassie 1, and the Asian specimens from India: Hathnora (Narmada), from China: Hexian, Dali, *Sinanthropus* III, XI and XII (from Zhoukoudian Lower Cave) and from the Idonesian Java island: Ngandong 6 and 12 and Sangiran 17.

3. Reconstitution methods

3.1. The Yunxian fossils

Because the two Yunxian skulls were deformed during their fossilization process, we carried out a virtual reconstruction using 3D virtual imaging techniques of the Yunxian II cranium which was the least damaged (Li et al., 2004; Vialet et al., 2005, 2008). First, the different types of damage were described (plastic deformation, breakage, destruction of bone…). Then, including observation done on the inner parts of the skull using data from Computer-Tomography (CT), the overall diagenetic history was reconstituted. Third, a comparison, by morphometrics, between the Yunxian specimen and Asian fossils was made in order to determine the least damaged parts of the Yunxian II cranium. On the basis of the results of these analyses, a reconstruction of the fossil has been made. The modifications to the vault were carried out using a global interactive deformation technique (with *Surfacer V9.08 Imageware®* and *RapidForm 2004 Inus Technology®* software) applied to a preliminary 3D reconstruction of the skull that had been created by surface triangulation using the *Mimics V 7.1 Materialise®* software (Fig. 2). To summarise, the left maxillary bone and the nasal cavity were restored and the missing parts of the face were completed using the well-preserved left cheek bone from the Yunxian I skull and mirrored it on both sides of Yunxian II. This reconstruction has resolved two important problems for the Yunxian II skull. First, the sagittal convexity of the frontal bone, because of its damage, was hard to estimate although it appears as an important character to evaluate really the degree of evolution of hominid fossils. Thanks to the CT data, it was possible to understand how the damage occurred on this part of the Yunxian II skull. Comparisons by morphometrics have also allowed the determination of the original convexity of the frontal bone. Based on this information, the reconstruction of the frontal part is valid. If the convexity was stronger, the conclusions about the Yunxian II skull would have been different. Moreover, concerning the face, the reconstruction of the specimen, using the cheek bone of the Yunxian I skull, delivered a much more complete fossil.

3.2. The Nankin fossils

Manual reconstructions of the Nankin 1 specimen, putting the three bone fragments in connection, were carried out by Liu et al. (2005), Lu (1996) and Wu et al. (2002). These teams have experienced the same difficulty to establish the anatomical connections between the three fragments: Nankin 1a with Nankin 1b (connection between the anterior and posterior parts of the left parietal) and Nankin 1b with Nankin 1c (connection between the occipital and posterior fragment of the right parietal bone). The reconstructions obtained are different for the main dimensions of the skull and the endocranial volume. At that time, no doubt has been expressed about the membership of these three fragments for the same individual. For the first time, CT data allowed us to test this hypothesis. Indeed, the density values were measured passing through the three bone fragments (Fig. 3). The values recorded for the frontal and the occipital bones (Nankin 1a and 1b) are really higher than those measured for the right fragment of
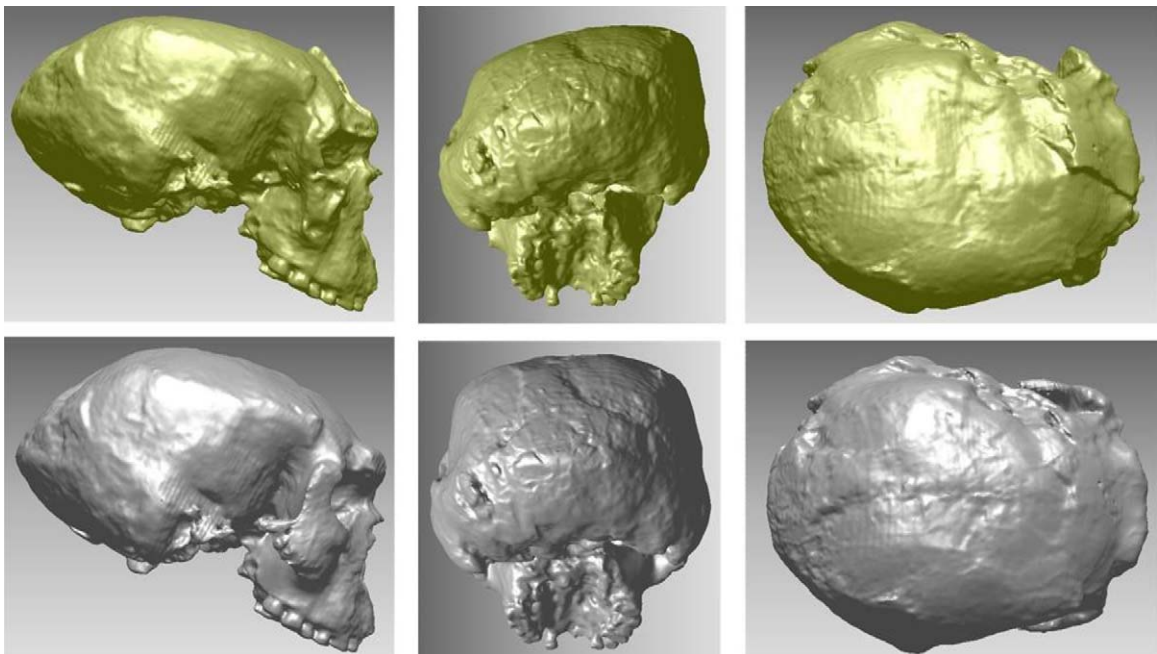

Fig. 2. Virtual reconstruction of the Yunxian II skull (above, in yellow: the specimen deformed, as it was discovered; bottom, in grey: the specimen as it was virtually reconstructed), from left to right: right lateral view, posterior view, superior view.
Fig. 2. Reconstitution virtuelle du crâne de Yunxian II (en haut, en jaune : le spécimen déformé, tel qu'il a été découvert ; en bas, en gris : le spécimen virtuellement reconstitué) ; de gauche à droite : vue latérale droite, vue postérieure, vue supérieure.

Fig. 3. Observed values of density passing through the coronal plane of the frontal bone (Nankin 1a), at left, the transverse plane of the occipitoparietal bone (Nankin 1b), at the middle, and of the right parietal fragment (Nankin 1c), at right. The arrows indicate where the measurements of the density of the tissue were made measured in Hounsfield (H). The density range is mentioned at the bottom of each specimen.

Fig. 3. Mesures des coefficients d'atténuation (densité) au travers du plan coronal du frontal (Nankin 1a), à gauche, du plan transversal de l'occipitopariétal (Nankin 1b), au milieu, et de celui du fragment pariétal droit (Nankin 1c), à droite. Les flèches indiquent les prises de mesure de la densité des tissus traversés, mesurée en Hounsfiled (H). L'étendue des valeurs d'insité esr reportée au bas de chaque spécimen.

the parietal bone (Nankin 1c). The density values indicate the degree of mineralization of the bone resulting from the process of fossilization. Such a difference in density value between the Nankin 1a and 1b, in the one hand, and Nankin 1c, in the other hand, may indicate that the bones have fossilized in distinct conditions and/or that they belonged to different individuals. A new reconstruction of the Nankin 1 specimen is underway, taking into account these unpublished data.

The face of Nankin 1, formed by a nearly complete frontal bone, the left cheek bone and most part of the left maxillary, is less problematic and can be reconstructed. In order to complete the missing parts of the face of Nankin 1, the mid-sagittal plane (passing through conventional landmarks such as Nasion, Bregma and anatomical entities such as the frontal crest and the sagittal suture) were used as the axis of symmetry and a mirror image of the left side of the face was performed using the *Rapidform 2006 Inus Technology*® software (Fig. 4).
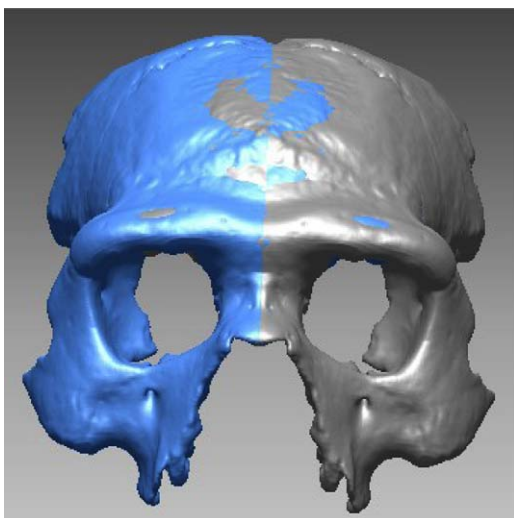

Fig. 4. Virtual reconstruction of the face of Nankin 1 by mirroring the left side. Original part in grey, mirror in blue.

Fig. 4. Reconstitution virtuelle de la face de Nankin 1 par image miroir de sa partie gauche. Partie originale en grise, image miroir en bleu.

4. Analysis methods

The methods used combined 2D and 3D morphometrics. Conventional measurements are from Martin (1914). For the Nankin fossil, the measurements were taken on 3D reconstruction using the *RapidForm 2006 Inus Technology*® software. The extension of its frontal sinuses was defined on the 2D CT slices and the volume was calculated using the *Mimics Version 13.1 Materialise*® software.

3D morphometric geometry based on Procrustes superpositions (i.e. generalized least square superimposition of all the specimens in the sample) and Principal Component Analysis generated by *Aps version 2.3* (Penin, 2000) on the covariance matrix from the Procrustes residuals were used to obtain a comprehensive treatment of the data after extracting the size. Landmaks were digitized with a *Micro-Scribe 3dx*. Due to the differences in the state of preservation between the fossils, 9 cranial and 18 facial landmarks were digitized on the Nankin 1 specimen, and, respectively, 10 and 21 landmarks on the Yunxian II skull. List of the cranial landmarks is described in Table 1 (for a description of the facial landmarks: Vialet, 2005).

5. Results

5.1. The Yunxian fossils

Based on the genuine specimen that we have made of the reconstructed Yunxian II skull, produced with the aid of a rapid prototyping system (Fig. 5), a standard anthropological study was done (de Lumley et al., 2008b). Results are summarized as follows. The Yunxian II skull appears surprisingly long and large relatively to the Asian *Homo erectus*, mainly at the biparietal level. While Yunxian II is not that high, its cranial base (i.e. under the Porion landmark) is well developped. Face is relatively high, narrow and orthognathous except in its alveolar part, which is prognathous. The nasal aperture is high and the palate is large and long. The supra-orbital torus, although its lateral parts are missing, is thick and prominent in the mid-sagittal area. Compared with a modern human's sample (Vialet, 2005), the proportions of the face of Yunxian II as well as its sensorial cavities and the angular conformation of its cheek bone can be integrated into the modern variability.

Table 1
Description of the landmarks digitized on the skull.
Tableau 1
Description des points de repère numérisés sur le crâne.

Landmark	Description	Yunxian IIr	Nankin 1
Conventional landmarks			
Na	Nasion		x
Br	Bregma	x	x
La	Lambda	x	
In	Inion	x	
Pt	Pterion	x	x
As	Asterion	x	
Po	Porion	x	
Incis par	Landmark at the *incisura parietalis* on the temporal bone	x	
FTP	Meeting point between the frontal, parietal and temporal bones		x
Specific landmarks			
½ P	Landmark on the superior border of the parietal bone, at one half of the border	x	x
½ STL	Intersection between the line from ½ P to ½ T and the superior temporal line	x	
½ T	Landmark on the superior border of the temporal bone, at one half of the border	x	
1/3 Na-Br	Landmark on the sagittal line between Na and Br, at the first third		x
2/3 Na-Br	Landmark on the sagittal line between Na and Br, at the second third		x
1/3 Br-Pt	Landmark on the left part of the coronal suture between Br and Pt, at the first third		x
2/3 Br-Pt	Landmark on the left part of the coronal suture between Br and Pt, at the second third		x
Total		10	9

However, the transversal angle of the zygomatic, passing through the body of the cheek bone between the maxillary and zygomatic processes, is closed in Yunxian II compared to modern humans. The inferior border of the zygomatic process of its maxillary is less arched and is more rooted in a lower position than modern humans.

Using 3D reconstruction, the endocranial volume was calculated. With a more reduced endocranial capacity (around 1050 cc) than previously thought, the reconstructed Yunxian II skull now falls within the *Homo erectus* range.

Generally speaking, the cranial pattern of Yunxian is close to the Asian *Homo erectus* in terms of sagittal flatness of vault, sloping forehead and lowness of the parietal bone and the occipital scale. By contrast, the mastoid por-

tion of the temporal bone is well developed and composed by a well-marked mastoid process. Note that this pattern is observed in more evolved hominids. The supra-mastoid and mastoid crests are little developed as well as the angular torus which is softly expressed. De Lumley et al. (2008a) suggested that the supra-mastoid crests were not very developed because of the well-marked mastoid process, which offers a large bone surface for the attachments of the rotatory muscles of the head. Compared to the Asian *Homo erectus*, those characters are peculiar in the Yunxian II specimen.

A Principal Component Analysis was generated (Fig. 6) from the covariance matrix calculated from the residuals of the Procrustes superimposition of 20 specimens represented by 10 landmarks on the temporal, parietal

Fig. 5. The original Yunxian skulls as they were discovered (at left: Yunxian I, at right: Yunxian II) and the prototype of the Yunxian II reconstructed skull (at the middle).
Fig. 5. Les crânes originaux de Yunxian, tels qu'ils ont été découverts (à gauche : Yunxian I, à droite : Yunxian II) et le prototype du crâne reconstitué de Yunxian II (au milieu).
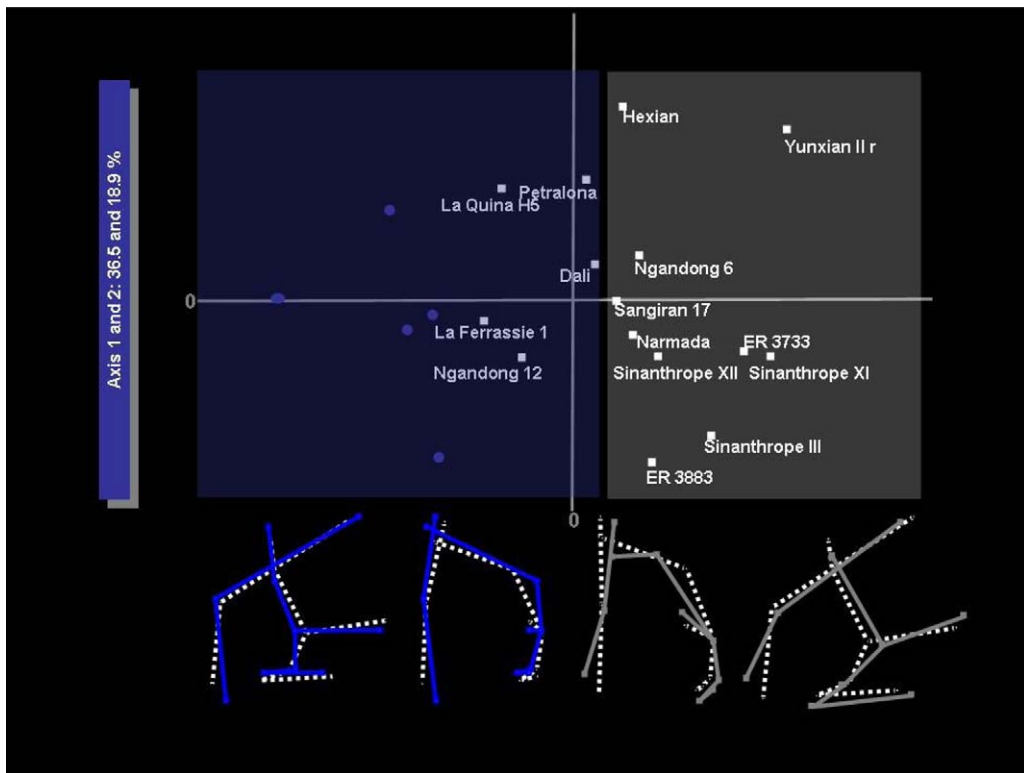
Fig. 6. PCA, two first axis (20 specimens, 10 landmarks). Extreme conformations of the posterior part of the skull along the first axis from left to right (in right lateral view and posterior view), full circles represent the modern human sample from the anthropological collection of the *Institut de paléontologie humaine*, ER3733 and ER3883 mean the specimens KNM-ER from Kenya.
Fig. 6. Analyse en composantes principales, Axes 1 et 2 (20 spécimens, 10 points-repères). Conformations extrêmes de la partie postérieure du crâne le long de l'axe 1 de la gauche vers la droite (en vue latérale droite et en vue postérieure). Les cercles pleins représentent l'échantillon d'hommes modernes de la collection anthropologique de l'Institut de paléontologie humaine, ER3733 et ER3883 représentent les spécimens KNM-ER du Kenya.

and occipital part of the skull. On the first axis, which represents 36.5% of the total variance, most of the fossils considered (i.e. *erectus*-like) are clearly different not only from the Neandertal and modern human samples but also from specimens such as Dali and Petralona. Those skulls and, among them the Yunxian II reconstructed cranium, are characterized by: a cranial flatness, an elongated temporal bone (in lateral view), a high location of the temporal lines and a low maximum cranial breath position (in posterior view). On the second axis (18.9%), the Hexian and the Yunxian II skulls are distinct from the rest of the sample due to their specific temporal conformation.

A new appraisal of the facial pattern of Yunxian II was done by morphometrics (Vialet, 2009). Results show that the cheek bone is more developed proportionally to the maxillary. The nasal spine and the upper part of the sagittal profile of the face is set back. The lateral wall of the nasal aperture is laterally projected so that an inflexion of the middle part of the face is present. The Yunxian face is different, not only from the Neandertal pattern, but also from the Middle Pleistocene specimens. The relative position of its zygomatic and maxillary bones is closer to the facial pattern of modern humans. This facial topography between the maxillary and the cheek bones, causing a depressed infra-orbital area of the maxillary, may be interpreted as an ancestral pattern which was sustained in modern humans.

5.2. The Nankin fossils

Thanks to the reconstruction of the Nankin 1 fossil, bilateral measures were included. Results from the standard anthropological study (Table 2) show that the Nankin 1 specimen is very close to the Asian *Homo erectus* in terms of frontal divergence (i.e. post-orbital constriction) and sagittal convexity of the frontal scale. However, the frontal bone of Nankin 1 is a little less constricted than the other specimens. It is less flat than Sangiran 17 but also less convex than Dali and Hexian. Conversely, the curvature of the anterior border of the parietal bone at the level of the coronal suture in Nankin 1 is peculiarly marked compared to all the other fossils considered. The relative flatness of the frontal scale and the strong convexity of its coronal border could result from the ectocranial lesion described by Shang and Trinkaus (2008).

The facial widths (Table 3) indicate that the Nankin 1 and Yunxian II reconstructed specimens are very close in proportions, although they are different in size (with the latter being larger than the former). The degree of protrusion of the Nasion is also very similar between the two fossils. The development of the frontal sinuses, which is different between Yunxian II and Nankin 1, is known to be variable. Indeed, variability in size and shape is evident between the right and the left frontal sinuses of Nankin 1.

Table 2
Metrics of the frontal bone (S17: Sangiran 17, SIII, SXI, SXII: Sinanthropes, YIIr: Yunxian II reconstructed; cast from the *Institut de paléontologie humaine*, Paris).
Tableau 2
Mesures de l'os frontal (S17 : Sangiran 17, SIII, SXI, SXII : Sinanthropes, YIIr : Yunxian II reconstitué ; les moulages proviennent de l'Institut de paléontologie humaine, Paris).

	Nankin 1	S17	SIII	Sin XI	Sin XII	YII r	Dali	Hexian
Nasion-Bregma Cord	94	104	103	104	111	105	113	99
Nasion-Bregma Arc	103	110	114	120	123	117	130	118
Index	91.26	94.55	90.35	86.67	90.24	89.74	86.92	83.90
Bregma-Coronion Cord	84	82	80	89	86	88	91	88
Bregma-Coronion Arc	106	90	90	103	96	96	105	105
Index	79.25	91.11	88.89	86.41	89.58	91.67	86.67	83.81
M9	88	98	87	92	94	106	105	101
M10	98	114	102	106	103	123	119	118
Index	89.80	85.96	85.29	86.79	91.26	86.18	88.24	85.59

Table 3
Metrics of the face of Yunxian II and Nankin 1 reconstructed. Conventional measures from Martin (1914) calculated in millimeters; (l) and (r) mean left and right.
Tableau 3
Mesures de la face de Yunxian II et de Nankin 1 reconstituées. Mesures conventionnelles d'après Martin (1914) calculées en millimètres ; (l) et (r) : respectivement gauche et droite.

	Nankin 1	Yunxian II
M43(1) bi-Fmo	96.9	113.2
M45(3) bi-Zo	62	65.8
M46 bi-Zm	98.5	115.5
M51 orbital width	46	51
Index M51/M43(1)	47.47	45.05
Index M45(3)/M43(1)	63.98	58.13
Index M43(1)/M46	101.65	102.03
M77 - Fmo (r)-N-Fmo (l) (°)	145.74	142.6
Frontal sinus height	8 (l) 10 (r)	20
Frontal sinus length	18 (l) 11 (r)	20
Frontal sinus width	14 (l) 11 (r)	19

Moreover, the development of the frontal sinus is related to the overall size of the individual. The supra-orbital torus is not as thick and prominent as on Yunxian II and a supra-toral groove is present, more pronounced in the lateral parts than in the mid-sagittal area. The temporal lines as well as the angular torus are well marked.

A Principal Component Analysis was generated (Fig. 7) from the covariance matrix calculated from the Procrustes residuals from the superimposition of 14 specimens represented by 9 landmarks on the frontal and parietal bones. On the first axis, which represents 49.2% of the total variance, Nankin 1 is closed to Yunxian II and Sangiran 17 because of its frontoparietal conformation and, particularly, its flatness. On the second axis, which expresses 18.9% of the total variance, Nankin 1 is distinct from the rest of the sample. It is because, in this specimen, the Nasion is protruding and the convexity of the coronal suture is peculiarly marked.

A previous study (Vialet, 2005) characterized the facial peculiarity of Nanjing 1 as the upper part of its cheek bone is in a backward position and its lower part is projected forward making a depressed infra-orbital region. Compared to Yunxian II, the cheek bone of Nankin 1 is in a more anterior position relative to the maxillary; the inferior border of the zygomatic process of the latter is clearly arched and it is rooted in a higher position.

6. Discussion

The Yunxian II and Nankin 1 skulls present a unique combination of features. The Yunxian II skull is large, elongated and low, and its endocranial capacity is within the *Homo erectus* range. Conversely, its mastoid region is surprisingly well individualized. Its superstructures and muscular attachments are not very marked except the supra-orbital torus which is thick and prominent. No true *angular torus* is developed. Although its face is larger in all measures, its pattern is close to modern humans in the proportions of sensory cavities and relative development and location between the maxillary and the cheek bone.

The Nankin 1 hominid is more gracile. Generally speaking, this specimen is *Homo erectus*-like: the anterior part of the skull is relatively flat (above all the frontal scale),
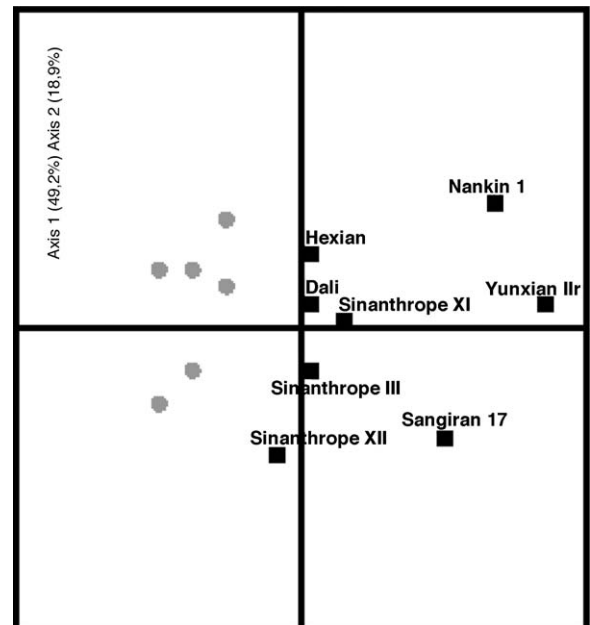

Fig. 7. PCA, two first axis (14 specimens, 9 landmarks on the frontoparietal bones). Full circles represent the modern human sample.
Fig. 7. Analyse en composantes principales (14 spécimens, 9 points-repères sur le frontopariétal), Axes 1 et 2. Les cercles pleins correspondent à l'échantillon d'hommes modernes.

the post-orbital constriction is marked and the superstructures and muscular attachments are well developed. By contrast, the coronal suture is surprisingly convex and the face is peculiar with the cheek bone that declines infero-anteriorly. Moreover, the inferior border of the zygomatic is rooted in a high position on the maxillary and forms a clearly arched maxillary crest. This disposition, including an antero-laterally projected nasal wall, causes a depressed infra-orbital area. This concavity of the infra-orbital area of the maxillary together with the presence of a well-marked maxillary crest on the inferior border of the zygomatic process was first described as close to modern humans by Weidenreich (1943) on the Chinese fossils from the Zhoukoudian Lower Cave (Vialet, 2004).

Results of this new anthropological analysis, managed on the reconstructions of the Yunxian II and Nankin 1 skulls, confirm the assignment of those specimens to *Homo erectus* as shown in previous studies (de Lumley et al., 2008a; Liu et al., 2005). However, even if the variability within the *Homo erectus* species is well known (Anton, 2002; Bräuer and Mbua, 1992; Grimaud-Hervé et al., 2002; Kidder and Durband, 2004; Rightmire, 1990; Schwartz and Tattersall, 2000; Terhune et al., 2007; Wu, 1995), the allocation of Yunxian II and Nankin 1 fossils to *Homo erectus* inflates the boundaries of this species.

7. Conclusion

The fossils of Yunxian and Nankin from China constitute appropriate examples to demonstrate the possibilities offered by the 3D virtual imaging techniques applied on human palaeontology. Computer tomography, which is the first step in the process of 3D virtual imaging techniques, enables to assess the diagenetic history of the fossils with more accuracy. Most subjects of discussion can be solved such as the degree of sagittal curvature of the frontal scale, in the case of the Yunxian II specimen, and the membership of the three bone fragments in the same skull, in the case of Nankin 1. Unpublished features can be studied such as the frontal sinuses and the endocranial capacity.

In a second time, the virtual reconstructions deliver more comprehensive fossils that are the subject of further analysis. Thus, for the first time, cranial as well as facial patterns have been studied on the Yunxian II skull and bilateral widths were measured on Nankin 1. Results show that Yunxian II and Nankin 1 specimens present an *erectus*-like cranial pattern while their cranial superstructures and muscular attachments are diversely expressed (poorly developed, on the former, except the supra-orbital torus, and more marked, on the latter, with a true angular torus). The facial features are also diverse while showing a pattern very close to modern humans which can be considered as the ancestral condition.

Thus, some morphological differences are well expressed between the Yunxian II and the Nankin 1 fossils. This is why assigning them to *Homo erectus* will increase the variability within this species. This exciting question, which has been debated for a long time, needs further investigations.

References

Anton, S.C., 2002. Evolutionary significance of cranial variation in Asian *Homo erectus*. Am. J. Phys. Anthropol. 118, 301–323.

Balzeau, A., Rougier, H., 2010. Is the suprainiac fossa a Neandertal autapomorphy? A complementary external and internal investigation. J. Hum. Evol. 58 (1), 1–22.

Balzeau, A., Jacob, T., Indriati, E., 2002. Structures crâniennes internes de l'*Homo erectus* Sambungmacan 1 (Java, Indonésie). C. R. Palevol 1, 1–7.

Bayle, P., Braga, J., Mazurier, A., Macchiarelli, R., 2009. Dental developmental pattern of the Neanderthal child from Roc de Marsal: a high-resolution 3D analysis. J. Hum. Evol. 56, 66–75.

Berge, C., Goularas, D., 2010. A new reconstruction of Sts 14 pelvis (*Australopithecus africanus*) from computed tomography and three-dimensional modeling techniques. J. Hum. Evol. 58 (3), 262–272.

Bräuer, G., Mbua, E., 1992. *Homo erectus* features used in cladistics and their variability in Asian and African hominids. J. Hum. Evol. 22, 79–108.

Braun, M., 1996. Applications de la scanographie à RX et de l'imagerie virtuelle en paléontologie humaine, PhD report. Muséum national d'histoire naturelle, Paris, France, 213 p.

Bruner, E., Manzi, G., 2008. Paleoneurology of an "early" Neandertal: endocranial size, shape, and features of Saccopastore 1. J. Hum. Evol. 54, 729–742.

Chen, T., Yang, Q., Hu, Y., Bao, W., Li, I., 1997. ESR dating of tooth enamel from Yunxian *Homo erectus* site, China. Quaternary Sci. Rev. 16, 455–458.

Conroy, G.C., Weber, G.W., Seidler, H., Recheis, W., Zur Nedden, D., Haile Mariam, J., 2000. Endocranial capacity of the Bodo cranium determined from three-dimensional computed tomography. Am. J. Phys. Anthropol. 113 (1), 111–118.

de Lumley, H., Li, T., 2008. Le site de l'Homme de Yunxian. Quyuanhekou, Qingqu, Yunxian, Province du Hubei. CNRS éditions et éditions Recherche sur les Civilisations, 587 p.

de Lumley, H., Khatib, S., Mestour, B., Gattacceca, J., Faure, O., Rochette, P., Vadeboin, F., Feng, X., 2008a. Étude du paléomagnétisme du site de l'Homme de Yunxian. In: de Lumley, H., Li, T., (Eds), Le site de l'Homme de Yunxian. Quyuanhekou, Qingqu, Yunxian, Province du Hubei, CNRS éditions et éditions Recherche sur les Civilisations, pp. 185–236.

de Lumley, M.A., Grimaud-Hervé, D., Li, T., Feng, X., Wang, Z., 2008b. Les crânes d'*Homo erectus* du site de l'Homme de Yunxian. In: de Lumley and Li, T., (Ed.) Le site de l'Homme de Yunxian. Quyuanhekou, Qingqu, Yunxian, Province du Hubei. CNRS éditions et éditions Recherche sur les Civilisations, pp. 381–466.

Etler, D., Li, T., 1994. New archaic human fossil discoveries in China and their bearing on hominid species definition during the Middle Pleistocene. In: Corruccini, R.S., Ciochon, R.L. (Eds.), Integrative Paths to the Past, Paleoanthropological Advances in honor of F. Clark Howell. Englewood Cliffs, pp. 639–675.

Falk, D., Hildebolt, C., Smith, K., Morwood, M.J., Sutikna, T., Jatmiko, Saptomo, E.W., Prior, F., 2009. LB1's virtual endocast, microcephaly, and hominin brain evolution. J. Hum. Evol. 57, 597–607.

Gilbert, W.H., Asfaw, B., *Homo erectus*. Pleistocene evidence from the Middle Awash, Ethiopia. University of California Press. 480 p.

Grimaud-Hervé, D., Marchal, F., Vialet, A., Détroit, F., 2002. Le deuxième Homme en Afrique : *Homo ergaster*, *Homo erectus*. Collection Paléontologie Humaine 4, Artcom-Errance, Paris, pp. 257.

Guipert, G., Mafart, B., Tuffreau, A., de Lumley, M.A., 2007. 3D reconstruction and study of a new late Middle Pleistocene Hominid: Biache-Saint-Vaast 2, Nord France. Am. J. Phys. Anthropol. Suppl. 44, 121–122.

Hill, C.A., Richtsmeier, J.T., 2008. A quantitative method for the evaluation of three-dimensional structure of temporal bone pneumatization. J. Hum. Evol. 55, 682–690.

Kidder, J.H., Durband, A.C., 2004. A re-evaluation of the metric diversity within *Homo erectus*. J. Hum. Evol. 46, 297–313.

Li, T., Etler, D.A., 1992. New Middle Pleistocene hominid crania from Yunxian in China. Nature 357, 405–407.

Li, T., Feng, X., 2001. The Yunxian man. Wuhan (China). Scientific and technological publisher of Hubei.

Li, T., Vialet, A., Liao, M., Feng, X., Li, W., 2004. Preliminary three dimensional reconstruction of the Yunxian II cranium. Acta Anthropologica Sinica 23 (Suppl.), 1–21.

Liu, W., Zhang, Y., Wu, X., 2005. Middle Pleistocene human cranium from Tangshan (Nanjing). Southeast China: a new reconstruction and comparisons with *Homo erectus* from Eurasia and Africa. Am. J. Phys. Anthropol. 127 (3), 253–262.

Lu, Z., 1996. Locality of the Nanjing man fossils 1993-1994. Cultural Relics Publishing House, Beijing, 306 p.

Macchiarelli, R., Bondioli, L., Galichon, V., Tobias, P.V., 1999. Hip bone trabecular architecture shows uniquely distinctive locomotor behaviour in South African *Australopithecines*. J. Hum. Evol. 36 (2), 211–232.

Mafart, B., Delingette, H., 2002. Colloquium: "Three-Dimensional Imaging in Paleoanthropology and Prehistoric Archeology".Archaeopress. British Archaeological Series 1049. Actes du XIVe Congrès UISPP, 108 p.

Mafart, B., Guipert, G., Alliez-Philip, C., Brau, J.J., 2007. Virtual reconstitution and new paleopathological study of the Magdalenian skull of Rochereil. C. R. Palevol. 6, 569–579.

Manzi, G., Bruner, E., Caprasecca, S., Gualdi, G., Passarello, P., 2001. CT-scanning and virtual reproduction of the Saccopastore Neandertal crania. Rivista di Antropologia 79, 61–72.

Martin, R., 1914. Lehrbuch der Anthropologie in systematischer Darstellung mit besonderer Berucksichtigung der anthropologischen Methoden. Jena: Verlag von Gustav Fisher.

Olejniczak, A.J., Smith, T.M., Feeney, R.N.M., Macchiarelli, R., Mazurier, A., Bondioli, L., Rosas, A., Fortea, J., de la Rasilla, M., Garcia-Tabernero, A., Radovčić, J., Skinner, M.M., Toussaint, M., Hublin, J.J., 2008. Dental tissue proportions and enamel thickness in Neandertal and modern human molars. J. Hum. Evol. 55 (1), 12–23.

Penin, X., 2000. Exploration de la variabilité de formes faciales par les composantes de conformation. J. Edgewise 41, 39–54.

Ponce de Leon, M.S., Zollikofer, C.P.E., 1999. New evidence from Le Moustier 1: computer-assisted reconstruction and morphometry of the skull. Anat. Record 254, 474–489.

Poza-Rey, E.M., Arsuaga, J.L., 2009. Reconstitution 3D par Computerized-tomography (CT) et endocrâne virtuel du crâne 5 du site de la Sima de Los Huesos (Atapuerca). L'Anthropologie 113 (1), 211–221.

Rightmire, G.P., 1990. The evolution of *Homo erectus*. A comparative anatomical studies of an extinct human species. Cambridge University Press, 260 p.

Schwartz, H.J., Tattersall, I., 2000. What constitutes *Homo erectus*? Acta Anthropologica Sinica 19 (Suppl.), 21–25.

Seidler, H., Falk, D., Stringer, C., Wilfing, H., Muller, G., Nedden, D., Weber, G., Reicheis, W., Arsuaga, J.L., 1997. A comparative study of stereolithographically modelled skulls of Petralona and Broken Hill: implications for future studies of Middle Pleistocene hominid evolution. J. Hum. Evol. 33, 691–703.

Semal, P., Toussaint, M., Maureille, B., Rougier, H., Crevecoeur, I., Balzeau, A., Bouchneb, L., Louryan, S., de Clerck, N., Rausin, L., 2005. Numérisation des restes humains néandertaliens belges. Préservation patrimoniale et exploitation scientifique. Notae Praehistoricae 25, 25–38.

Shang, H., Trinkaus, E., 2008. An ectocranial lesion on the Middle Pleistocene human cranium from Hulu Cave, Nanjing, China. Am. J. Phys. Anthropol. 135, 431–437.

Shang, H., Tong, H., Zhang, S., Chen, F., Trinkaus, E., 2007. An early modern human from Tianyuan Cave, Zhoukoudian, China. Proc. Nat. Am. Sci. 104, 6573–6578.

Spoor, F., Hublin, J.J., Braun, M., Zonneveld, F., 2003. The bony labyrinth of Neanderthals. J. Hum. Evol. 44, 141–165.

Sylvester, A.D., Merkl, B.C., Mahfouz, M.R., 2008. Assessing A.L. 288-1 femur length using computer-aided three-dimensional reconstruction. J. Hum. Evol. 55, 665–671.

Terhune, C.E., Kimbel, W.H., Lockwood, C.A., 2007. Variation and diversity in *Homo erectus*: a 3D geometric morphometric analysis of the temporal bone. J. Hum. Evol. 53, 41–60.

Thompson, J.L., Illerhaus, B., 1998. A new reconstruction of the Le Moustier 1 skull and investigation of internal structures using 3-D-μCT data. J. Hum. Evol. 35, 647–665.

Vialet, A., 2004. L'utilisation de la face des *Homo erectus* comme argument taxinomique. Br. Archaeol. Res. S1272, 149–156.

Vialet, A., 2005. La face supérieure et moyenne des hominidés fossiles depuis le Pléistocène inférieur récent, PhD report. Muséum national d'Histoire naturelle, Paris, 290 p.

Vialet, A., 2009. L'évolution de l'homme en Eurasie : nouveaux fossiles, nouveaux outils d'analyse. L'Anthropologie 113, 245–254.

Vialet, A., Li, T., Grimaud-Hervé, D., de Lumley, M.A., Liao, M., Feng, X., 2005. Proposition de reconstitution du deuxième crâne d'*Homo erectus* de Yunxian (Chine). C. R. Palevol. 4, 265–274.

Vialet, A., Li, T., Feng, X., Liao, M., 2008. Reconstitution du crâne de l'Homme de Yunxian par imagerie tridimensionnelle. In: de Lumley, H., Li, T. (Eds.), Le site de l'Homme de Yunxian. Quyuanhekou, Qingqu, Yunxian, Province du Hubei. CNRS éditions et éditions Recherche sur les Civilisations, pp. 365–381.

Weidenreich, F., 1943. The skull of *Sinanthropus pekinensis*. A comparative study on a primitive hominid skull. Paleontologica Sinica New Series D 10, 1–291.

Wu, R., Li, X., Wu, X., Mu, X., 2002. The Nanjing *Homo erectus* and its living environment. Nanjing Jiangsu Science and Technology Publishing House, pp. 316.

Wu, X., 1995. Evolution and dispersal. In: Wu, X., Poirier, F.E. (Eds.), Human Evolution in China. A Metric Description of the Fossils and a Review of the Sites. Oxford University Press, pp. 234–240.

Wu, X., Liu, W., Dong, W., Que, J., Wang, Y., 2008. The brain morphology of *Homo* Liujiang cranium fossil by three-dimensional computed tomography. Chinese Sci. Bull. 23, 1–7.

Xing, S., Zhou, M., Liu, W., 2009. Crown morphology and variation of the lower premolars of Zhoukoudian *Homo erectus*. Chinese Sci. Bull. 54, 3905–3915.

Zhu, R., An, Z., Potts, R., Hoffman, K.A., 2003. Magnetostratigraphic dating of early humans in China. Earth Sci. Rev. 61, 341–343.

Zollikofer, C.P.E., Ponce de Leon, M.S., Martin, R.D., Stucki, P., 1995. Neanderthal computer skulls. Nature 375, 283–285.

Zollikofer, C.P.E., Ponce de León, M.S., Lieberman, D.E., Guy, F., Pilbeam, D., Likius, A., Mackaye, H.T., Vignaud, P., Brunet, M., 2005. Virtual cranial reconstruction of *Sahelanthropus tchadensis*. Nature 434, 755–759.